Volume 6 · No. 8 – April 23 2010

D15063

NANO

www.small-journal.com

8/2010

Bionanosphere Lithography via Hierarchical Peptide Self-Assembly of Aromatic Triphenylalanine
H. S. Lee, S. O. Kim, et al.

small NANO MICRO

Nanolithography

Bionanosphere Lithography via Hierarchical Peptide Self-Assembly of Aromatic Triphenylalanine

Tae Hee Han, Taedong Ok, Jangbae Kim, Dong Ok Shin, Hyotcherl Ihee, Hee-Seung Lee, and Sang Ouk Kim**

***A** nanolithographic approach based on hierarchical peptide self-assembly is presented. An aromatic peptide of N-(t-Boc)-terminated triphenylalanine is designed from a structural motif for the β-amyloid associated with Alzheimer's disease. This peptide adopts a turnlike conformation with three phenyl rings oriented outward, which mediate intermolecular π–π stacking interactions and eventually facilitate highly crystalline bionanosphere assembly with both thermal and chemical stability. The self-assembled bionanospheres spontaneously pack into a hexagonal monolayer at the evaporating solvent edge, constituting evaporation-induced hierarchical self-assembly. Metal nanoparticle arrays or embossed Si nanoposts could be successfully created from the hexagonal bionanosphere array masks in conjunction with a conventional metal-evaporation or etching process. Our approach represents a bionanofabrication concept that biomolecular self-assembly is hierarchically directed to establish a straightforward nanolithography compatible with conventional device-fabrication processes.*

Keywords:
- bionanospheres
- nanolithography
- peptides
- self-assembly

1. Introduction

The self-assembly of biomolecular building blocks has attracted a great deal of attention as a powerful approach for designing novel, benign, nanometer-scale processing.[1] A number of biomolecules, including nucleic acids, peptides, proteins, and their derivatives, have been reported to self-assemble into shape-specific nanostructures, such as micelles, vesicles, fibers, networks, and many other morphologies.[1,2] Nevertheless, the utilization of biomolecular self-assembly has been mostly limited to biological or medicine-related fields so far.[3] Unlike the self-assembly of synthetic molecules,[4] biomolecularly assembled morphologies have revealed low thermal and chemical stabilities, such that their utilization in conjunction with a harsh conventional device-fabrication process has been rarely achieved. Furthermore, macroscale alignment and positioning of the biomolecularly assembled morphologies on a desired substrate surface constitutes another major obstacle for conventional device application. While several bionanofabrication approaches, such as nanoparticle array fabrication by using S-layer protein assembly[5] or surface nanopatterning by an atomic force microscopy (AFM) tip decorated with DNA molecules,[6] have been suggested, the development of bionanofabrication compatible with conventional device fabrication is still in its infancy.

Nanosphere lithography (NSL), in which a self-assembled monolayer of synthetic hard spheres is employed as a lithographic template, has been extensively exploited as a

[*] T. H. Han, D. O. Shin, Prof. S. O. Kim
Soft Nanomaterials National Research Laboratory
Department of Materials Science and Engineering
KAIST, Daejeon 305-701 (Republic of Korea)
E-mail: sangouk.kim@kaist.ac.kr
T. Ok, Prof. H.-S. Lee
Biomimetic Organic Laboratory
Department of Chemistry
KAIST, Daejeon 305-701 (Republic of Korea)
E-mail: hee-seung_lee@kaist.ac.kr
J. Kim, Prof. H. Ihee
Center for Time-Resolved Diffraction, Department of Chemistry
KAIST, Daejeon 305-701 (Republic of Korea)

Supporting Information is available on the WWW under http://www.small-journal.com or from the author.

DOI: 10.1002/smll.200902050

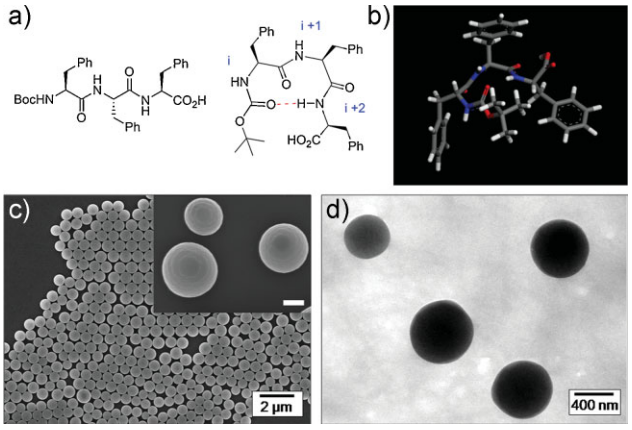

Figure 1. Triphenylalanine self-assembly into bionanospheres. a) Molecular structure of Boc-FFF and a mode of intramolecular ten-membered hydrogen bonding (shown with a red dashed line). b) Optimized conformation of a Boc-FFF molecule by quantum mechanical calculation (C gray, H white, O red, N blue). c) SEM and d) TEM images of Boc-FFF bionanospheres.

low-cost, inherently parallel, high-throughput fabrication technique for ordered micro/nanostructures.[7] To date, NSL has been successfully applied to, for example, highly sensitive surface-enhanced Raman scattering (SERS),[8] real-time chemical/biological sensors,[9] and so on. In this Full Paper, we demonstrate "bionanosphere lithography" as an alternative nanolithography method based on the self-assembly of aromatic peptides. In contrast to conventional NSL, which requires the laborious preparation of monodisperse silica or polymer hard spheres, our approach enables the straightforward assembly of biomolecules into a lithographic mask. We have obtained highly crystalline and thermally stable bionanospheres via the self-assembly of triphenylalanine (FFF) and exploited their close-packed monolayers for nanosphere lithography. The self-assembly of the peptide into nanospheres and the close packing of the generated nanospheres into a hexagonal monolayer occurred spontaneously during solvent evaporation on a silicon substrate, constituting evaporation-induced hierarchical self-assembly.[10] Taking advantage of the high thermal and chemical stabilities of the bionanosphere array mask, either hexagonally ordered metal nanoparticle arrays or embossed Si nanoposts were readily fabricated by selective deposition or by selective etching. Our approach represents a novel biomolecular design concept for hierarchical nanometer-scale assembly and offers a versatile route to biomaterial-based nanolithography compatible with the conventional device-fabrication process.

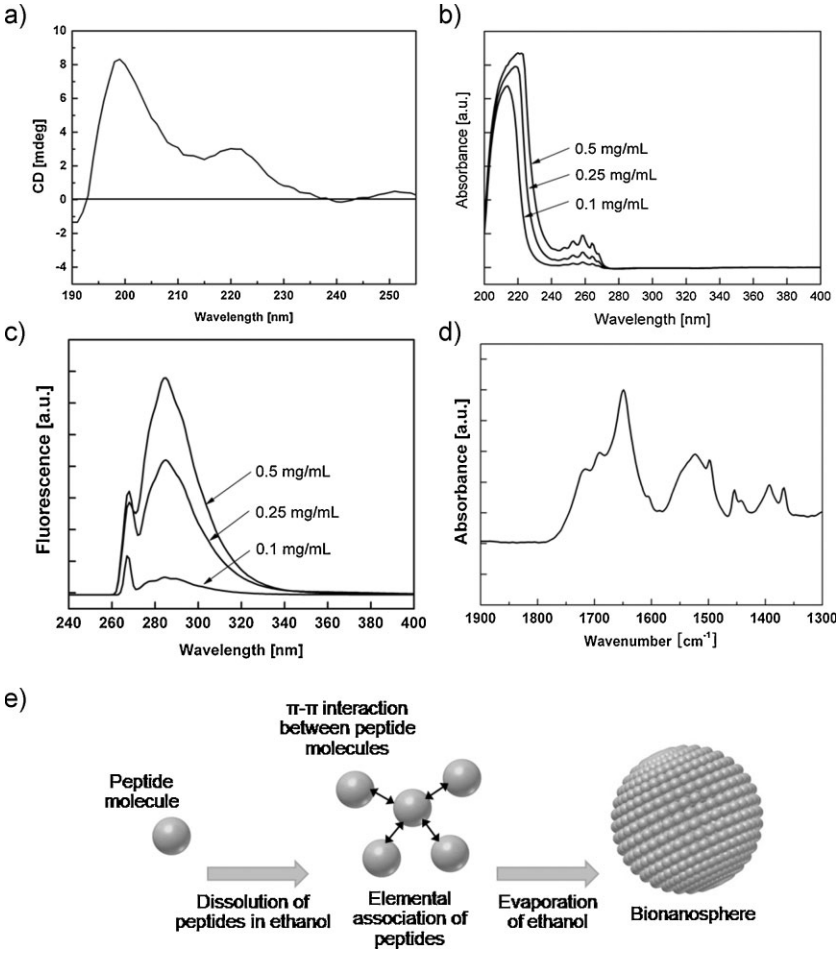

Figure 2. Spectroscopic analysis of the molecular interactions for a Boc-FFF assembly. a) CD spectrum, b) UV/Vis absorption, and c) florescence emission ($\lambda_{excitation} = 260$ nm) of dilute Boc-FFF solution. d) FT-IR spectrum of the dried bionanospheres. e) Proposed self-assembly mechanism. A phenyl ring of Boc-FFF undergoes $\pi-\pi$ stacking with a nearby phenyl ring from a neighboring molecule to facilitate assembly into a nanosphere morphology.

2. Results and Discussion

Figure 1a shows the molecular structure of the N-Boc-protected triphenylalanine (Boc-FFF) synthesized in this work. The N terminus is protected with a *t*-butyloxycarbonyl (Boc) group and the C terminus is a free carboxylic acid. This FFF derivative was synthesized with standard solution-phase chemistry and purified by recrystallization from acetonitrile[11] (see Supporting Information). The design of FFF was motivated by previous studies on diphenylalanine (FF), a well known structural motif for the β-amyloid associated with Alzheimer's disease.[12] The aromatic FF and its derivatives have been found to self-assemble into highly stable, one-dimensional nanometer-scale morphologies, such as nanotubes, nanowires, and nanoribbons, depending on their chemical structures, the type of their terminal functional groups, the assembly conditions, and so on.[12–21] Inter- and intra-molecular hydrogen bonding and aromatic $\pi-\pi$ stacking have been found to be the major molecular interactions driving its self-assembly behavior.[14,17,18,21] In this

work, Boc-FFF was designed to introduce an intramolecular ten-membered hydrogen bonding between the C=O of the carbamate group and N–H of the $(i+2)$ Phe residue into the aromatic peptide scaffold, as described in Figure 1a. The Boc-FFF is expected to adopt a turn-like conformation with three phenyl rings oriented outward, which is disallowed in FF derivatives (Figure 1b).[22] The outward phenyl rings mediate π–π stacking interactions with nearby phenyl rings from neighbors to facilitate the eventual assembly into nanosphere morphologies. Figure 1c shows a scanning electron microscopy (SEM) image of triphenylalanine bionanospheres left over on a silicon substrate upon evaporation from ethanol solution. Transmission electron microscopy (TEM) investigation verified that, unlike a hollow vesicular structure, the nanosphere cores were fully filled without void spaces (Figure 1d).

The molecular interactions involved in the self-assembly of Boc-FFF were investigated by spectroscopic analysis, including circular dichroism (CD), UV/Vis absorption/fluorescence spectroscopy, and Fourier-transform infrared (FT-IR) spectroscopy. Figure 2a shows the CD spectrum of a dilute ethanol solution of Boc-FFF. The two positive maxima at ≈200 and ≈220 nm indicate the π–π stacking of aromatic units, as frequently observed in the CD profiles for biomolecular self-assembly with β-turn conformation.[20] UV/Vis absorption and fluorescence spectroscopy for diluted solutions (Figure 2b and c) also support the existence of aromatic π–π stacking interactions.[20,23] The UV/Vis absorption spectrum in Figure 2b shows two peaks at 210 and 260 nm. The peak at 260 nm corresponds to the phenylalanine residues in proteins, while the peak at 210 nm arises from the existence of phenyl rings.[23] As shown in Figure 2c, the fluorescence spectrum shows a peak at 290 nm that corresponds to π–π interactions between phenyl units.[23] The FT-IR spectrum of the dried spherical Boc-FFF assembly exhibited a significant β-turn character based on the position of the amide I band at 1690 cm^{-1} and 1650 cm^{-1} (Figure 2d).[20,23] The peak at 1650 cm^{-1} was assigned to aperiodic secondary structures involving type I, II, VIa, and VII β-turns. The peak at 1690 cm^{-1} can be identified as a marker band for the β-turn conformations adopted by the molecules. The optimized geometry of Boc-FFF generated from a quantum-mechanical calculation at the AM1 level agreed well with the experimentally observed characteristic β-turn structure from FT-IR analysis (Figure 1b).[22] Meanwhile, dynamic light scattering (DLS) measurements detected no discrete particles in the ethanol solution of Boc-FFF. This demonstrates that the self-assembly of Boc-FFF into bionanospheres did not occur in the dilute ethanol solution but instead occurred during solvent evaporation. Taken together, Boc-FFF molecules with β-turn secondary structures exist as elementary aggregates with π–π interactions among the phenyl groups in a solution and subsequently self-assemble into crystalline spheres upon solvent evaporation (Figure 2e).

Figure 3a shows a thermogravimetric analysis (TGA) thermogram of Boc-FFF bionanospheres. Unlike usual biomaterials, the aromatic Boc-FFF nanospheres have a relatively high thermal stability. A weight loss of about 30% occurred from ≈170–250 °C, which presumably can be attributed to the gradual thermal release of peptide molecules.[17,24] The major

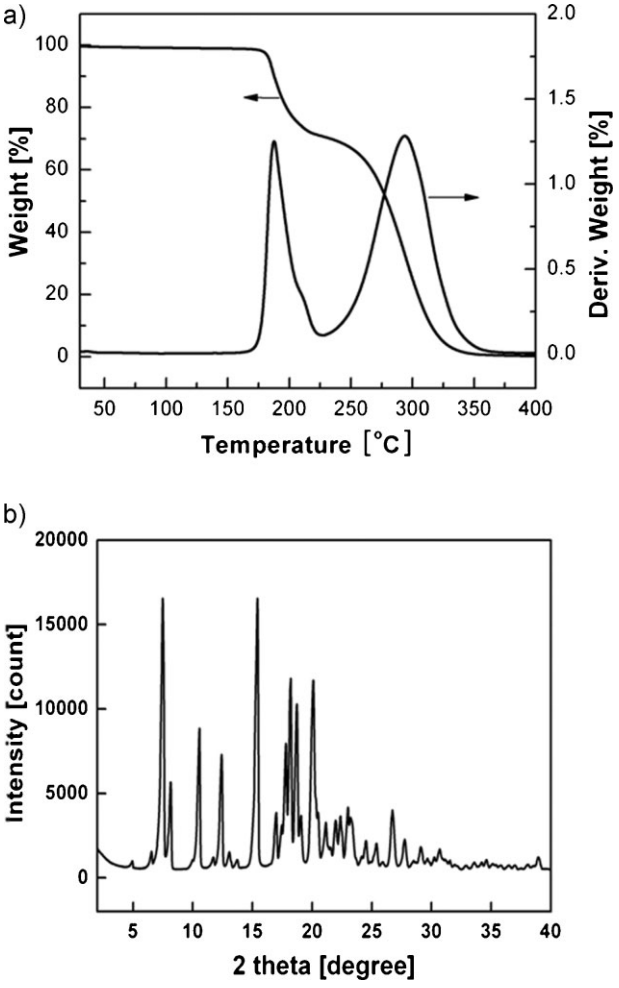

Figure 3. a) TGA plot of bionanospheres showing high thermal stability up to 250 °C. b) Powder XRD of a bionanosphere demonstrating a high crystallinity.

weight loss for the remaining 70% that was caused by thermal degradation occurred at above ≈250 °C. This high thermal stability of the bionanospheres is due to the highly crystalline assembly of aromatic Boc-FFF. As shown in Figure 3b, X-ray diffraction (XRD) measurements of the bionanospheres showed a high degree of crystallinity.

Figure 4a schematically illustrates the evaporation-induced hierarchical self-assembly of Boc-FFF. Upon the drying of a dispensed ethanol solution drop under humid air, Boc-FFF molecules spontaneously assembled into bionanospheres, which were subsequently close packed into two-dimensional colloidal arrays following the mechanisms of ''convective assembly'' and ''capillary-force-induced aggregation.''[25] As the ethanol evaporated, a convective flux was built up inside the solution drop towards the solution-drop edge due to solvent depletion at the evaporating-solution edge. This convective flow carried the self-assembled Boc-FFF bionanospheres to the solution edge. The bionanospheres transferred to the solution edge experienced attractive capillary immersion interactions with their neighboring bionanospheres, which were caused by the remaining solvent wetting the film. To minimize the capillary force due to this thin wetting film, bionanosphere

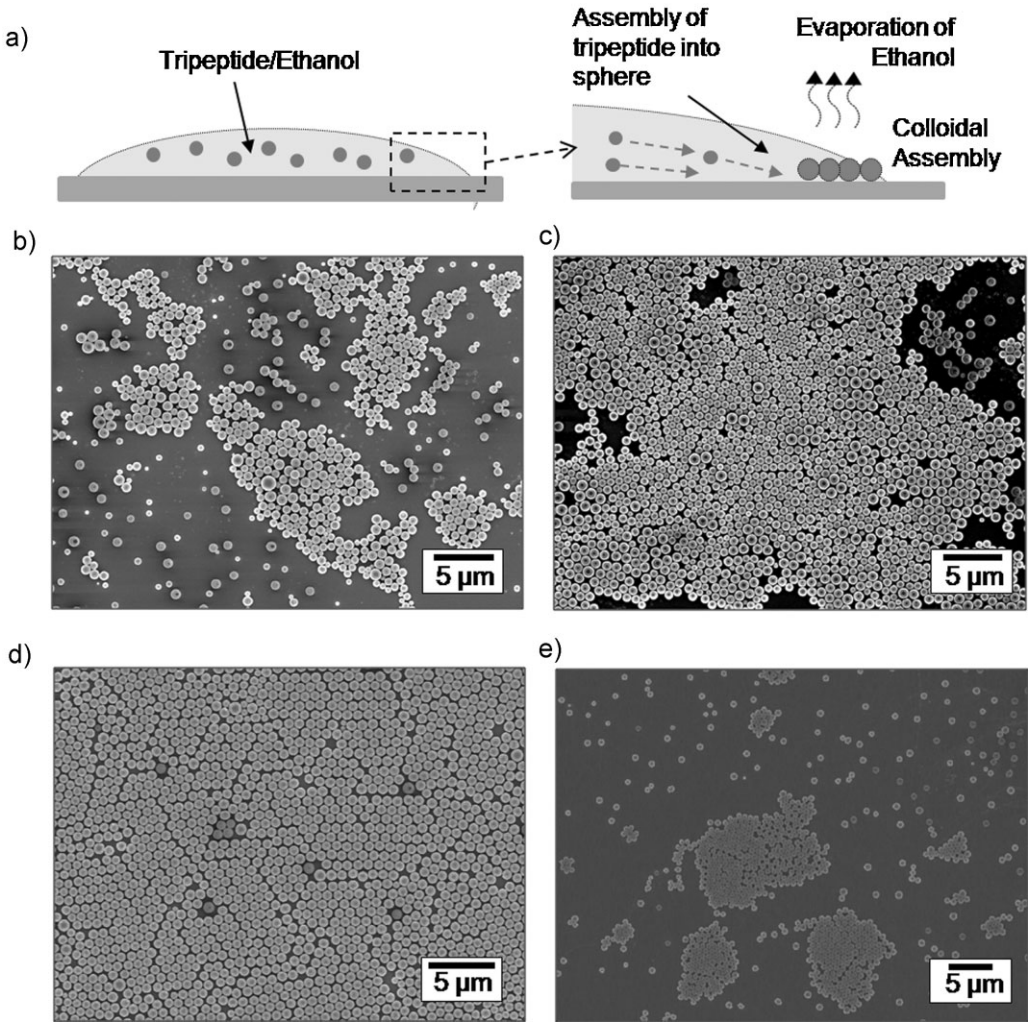

Figure 4. Hierarchical self-assembly of Boc-FFF into a hexagonal bionanosphere array at various humidity conditions. a) Schematic illustration of hierarchical assembly into a hexagonal bionanosphere array. During evaporation of the ethanol, Boc-FFF molecules assemble into bionanospheres that close pack to form a hexagonal array. SEM images of bionanospheres at relative humidities of b) 40%, c) 50%, d) 60%, and e) 80%.

colloidal particles were forced to close pack, and, thus, the liquid–air interfacial area was minimized.

As demonstrated in the previous evaporation-induced self-assembly (EISA), a variety of environmental parameters can influence the self-assembly behavior. In our approach, humidity turned out to be a crucial parameter for the hierarchical self-assembly. The humidity controlled the evaporation rate of ethanol, and, therefore, the size distribution of bionanospheres and their subsequent hexagonal assembly. As shown in Figure 4b–e (40, 50, 60, and 80% relative humidity, respectively), variation in the humidity significantly influenced the size distribution of bionanosphere assembly and the degree of ordering of their colloidal assembly (Figure 5). Below a relative humidity of 50%, the size distribution of Boc-FFF nanospheres was fairly broad, as demonstrated in the histograms of Figure 5a and b. The close packing of such polydisperse nanospheres generated disordered arrangements. In contrast, at a higher relative humidity of 60 or 80%, the nanospheres became highly uniform. The slow evaporation of ethanol that occurred at the highly humid conditions created the monodisperse nanospheres. The close packing of monodisperse nanospheres generated a well ordered hexagonal monolayer, particularly at a humidity of 60%, as presented in Figure 4d. When the relative humidity was over 80%, the packing area of the colloidal particles decreased significantly. This reduced packing area could result from the Maragoni effect.[26] Due to the vast difference in surface tension between water (72 mN m^{-1}) and ethanol (22 mN m^{-1}), a surface-tension gradient could be built up at the interface of ethanol and condensed water.[26] Such Such Maragoni flow could transfer Boc-FFF molecules from ethanol to the water phase. Due to its higher volatility, ethanol evaporates more rapidly than condensed water, leaving behind condensed water containing Boc-FFF molecules in a small, limited area. The subsequent evaporation of water left behind only the ordered bionanosphere array within the limited area.

Figure 6a shows a hexagonal monolayer of Boc-FFF bionanospheres assembled at a humidity of 60% at room temperature. The fast Fourier transform of the SEM image (inset) clearly demonstrates a highly ordered hexagonal arrangement. We employed this bionanosphere array as a mask for selective deposition or selective etching. As shown in

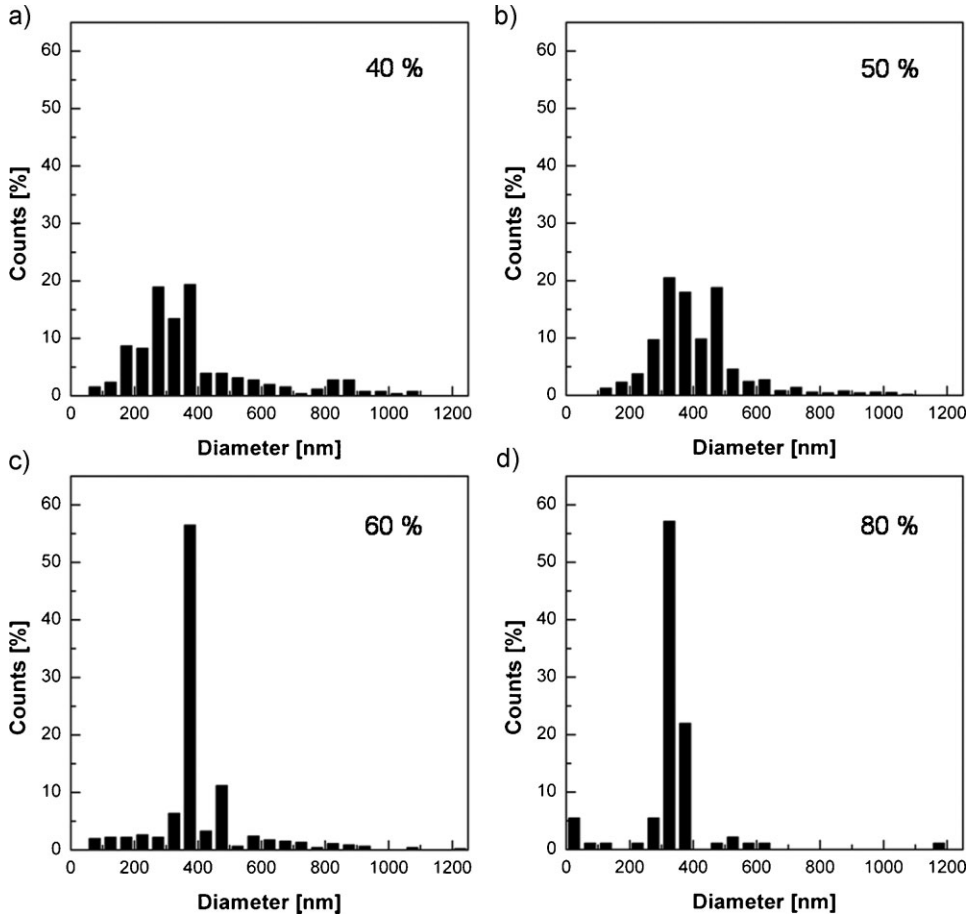

Figure 5. Histograms for the size distribution of bionanospheres at various humidity conditions: a) 40%, b) 50%, c) 60%, and d) 80%. The mean diameters of the spheres were approximately 379 nm, 399 nm, 397 nm, and 334 nm for (a)–(d), respectively.

Figure 6b, the thermal evaporation of aluminum (Al) over a bionanosphere array generated Al nanoparticle arrays. After metal deposition, the bionanosphere mask could be readily lifted off by mild ethanol washing. The deposited Al nanoparticles demonstrated a trigonal pyramid morphology with a side length of ≈260 nm and a height of ≈35 nm in the tilted SEM image of Figure 6c. The metal nanoarray prepared is potentially useful for localized surface plasmon resonance (LSPR) biosensors.[27] Figure 6d presents the tilted SEM image of a hexagonal silicon nanopost array produced by CF_4 reactive ion etching (RIE) (100 sccm, 100 W, 30 min) employing a Boc-FFF bionanosphere monolayer as an etching mask. While usual biomolecularly assembled structures consisting of poorly crystalline organic molecules could not effectively serve as a mask for RIE due to their low chemical resistance to etchant, the highly crystalline Boc-FFF bionanosphere array successfully played the role of an etching mask for the selective etching of the underlying silicon substrate.

3. Conclusions

We have demonstrated the hierarchical self-assembly of Boc-FFF peptide molecules into a hexagonal bionanosphere array on a substrate. We have designed a self-assembling peptide of Boc-FFF, inspired by a structural motif for the β-amyloid associated with Alzheimer's disease. We were able to fabricate periodic metal nanoparticle arrays and Si nanopost arrays, employing monolayered bionanosphere arrays as lithographic masks. Our bionanofabrication concept presents a novel approach to the design of biomolecular assembly for well defined nanometer-scale morphology, to position the nanomaterials in ordered arrays, and to develop a straightforward lithography exploiting hierarchical biomolecular self-assembly.

4. Experimental Section

Synthesis of Boc-FFF and the quantum-mechanical calculation: General synthetic details, including the instrumentation and methods, are given in the Supporting Information. The N-(*t*-butyloxycarbonyl)-protected triphenylalanine (Boc-Phe-Phe-Phe-OH) Boc-FFF was synthesized by standard solution-phase chemistry. N-Boc-Phe-OH monomer was purchased from Novabiochem. Chemicals of the highest purity grade, N,N-dimethylformamide (DMF), O-benzotriazole-N,N,N′,N′-tetramethyluroniumhexafluorophosphate (HBTU), hydroxybenzo-triazole (HOBt), and

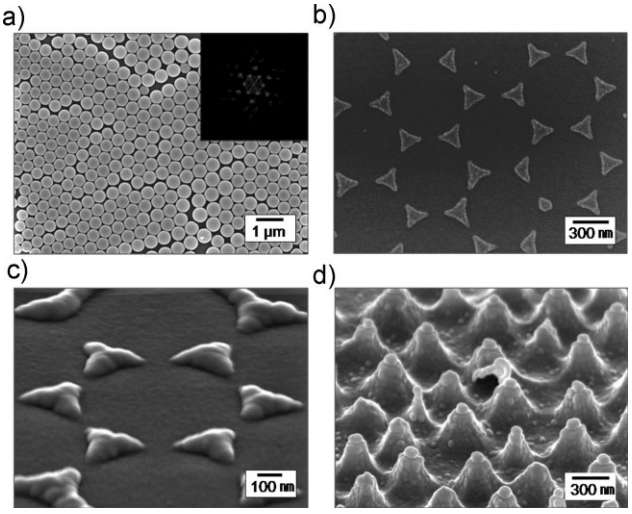

Figure 6. Fabrication of ordered nanostructures utilizing hexagonal bionanosphere templates. a) Close-packed monolayer of bionanospheres on a silicon substrate. The fast-Fourier-transform image (inset) represents hexagonally ordered structures. SEM images of Al nanoparticle arrays b) in plane view and c) with a tilted view. After Al deposition (35-nm thickness) by thermal evaporation and the subsequent lift off, hexagonally ordered Al trigonal pyramid arrays were readily fabricated. d) SEM image of a Si nanopost array prepared by CF_4 RIE with a bionanosphere array as an etching mask.

diisopropylethylamine (DIEA), were purchased from Sigma-Aldrich for the synthesis of triphenylalanine and were further purified. Water was deionized by using Milipore MilliQ.

N-Boc-protected phenylalanine was coupled with a previously prepared diphenylalanine fragment (C-benzyl protected) using HBTU, HOBt, and DIEA in anhydrous DMF at room temperature to obtain Boc-Phe-Phe-Phe-OBn. Hydrogenolysis of the benzyl ester provided the crude carboxylic acid, which was recrystallized from CH_3CN to yield Boc-FFF. The conformation optimization of a triphenylalanine molecule was performed at the AM1 level using the Gaussian 03 program package. No geometrical constraints were imposed on the triphenylalanine molecule during the optimization of conformation.

Fabrication of Boc-FFF bionanospheres: A predetermined amount of Boc-FFF was completely dissolved in ethanol (peptide concentration $\approx$0.1–20 mg mL^{-1}). A drop of Boc-FFF solution was deposited on a silicon substrate, which was subsequently maintained in a humidity-controlled environment for solvent evaporation. The evaporation rate of solvent was controlled by a stream of humid air (mobile gas: N_2) at room temperature.

Fabrication of hexagonal metal nanoparticle arrays and Si nanopost arrays: The Al nanoparticle arrays were produced by thermal evaporation of a 35-nm-thick Al layer over a hexagonal colloidal monolayer of Boc-FFF bionanospheres. After metal deposition, the Boc-FFF bionanospheres were completely removed by sonication in ethanol (JAC 2010, 65 W, 40kHz; Ko Do Tech.). The embossed Si nanopost arrays were prepared by RIE with CF_4 gas (100 sccm, 100W) using Boc-FFF bionanosphere arrays as an etching mask. The residual colloidal mask was removed by dissolution in ethanol.

Characterization: Morphological investigations were performed with a field-emission SEM system (FESEM; Hitachi S-4800 SEM, Japan) and a high-resolution TEM system (HRTEM; Philips Tecnai F20). Molecular interactions for the assembly of Boc-FFF were examined by spectroscopy analysis. The UV/Vis spectroscopy of the diluted Boc-FFF solution was obtained by a UV/Vis near-infrared (UV/Vis-NIR) scanning spectrophotometer (Shimadzu, UV-3101 PC). A 1.0-cm-path-length quartz cuvettes sample holder was used. The fluorescence intensity was measured by excitation at 265 nm (slit width of 5 nm) with a spectrofluorophotometer (Shimadzu, RF-5301PC). The CD spectrum was recorded on a J-815 Spectropolarimeter (150-L Type, Jasco Inc., Japan). Samples were dissolved in ethanol (0.5 mg mL^{-1}) and loaded into a 1-mm quartz cuvette. A spectrum was obtained from 190 to 260 nm. FT-IR (Bruker Optiks, IFS66V/S & HYPERION 300) spectra of dried Boc-FFF bionanospheres were obtained from KBr pellet samples. The crystallinity of the bionanospheres was characterized by means of powder XRD with CuKα radiation on a D/Max 2500 X-ray diffractometer (Rikagu, Japan). The thermal stability was examined by a Q500 thermogravimetric analyzer (TA Instruments, USA). The TGA measurements were carried out from 30 to 400 °C at a heating rate of 20 °C min^{-1} under a stream of nitrogen (purging rate: 60 mL min^{-1}). The DLS measurements were performed with a BI-200SM (Brookhaven Instruments Co., USA) with a 532-nm laser source at 25 °C. Image analysis of the bionanosphere array for size determination was performed with Matrox Inspector software version 2.1 (Matrox Electronic System Ltd., Canada).

Acknowledgements

This work was supported by the National Research Laboratory Program (RoA-2008-000-20057-0), National Research Foundation of Korea Grant (2008-0062204,2009-0075849), Creative Research Initiatives (Center for Time-Resolved Diffraction), and the Fundamental R&D Program for Core Technology of Materials funded by the Korean government.

[1] S. Zhang, *Nat. Biotechnol.* **2003**, *21*, 1171; X. Gao, H. Matsui, *Adv. Mater.* **2005**, *17*, 2037.
[2] Y. He, T. Ye, C. Zhang, A. E. Ribbe, W. Jiang, C. Mao, *Nature* **2008**, *452*, 198; W. C. Pomerantz, V. M. Yuwono, C. L. Pizzey, J. D. Hartgerink, N. L. Abbott, S. H. Gellman, *Angew. Chem. Int. Ed.* **2008**, *47*, 1241; T. Koga, M. Higuchi, T. Kinoshita, N. Higashi, *Chem. Eur. J.* **2006**, *12*, 1360; H. Cui, T. Muraoka, A. G. Cheetham, S. I. Stupp, *Nano Lett.* **2009**, *9*, 945.
[3] A. Mahler, M. Reches, M. Rechter, S. Cohen, E. Gazit, *Adv. Mater.* **2006**, *18*, 1365; L. Aulisa, N. Forraz, C. McGuckin, J. D. Hartgerink, *Acta. Biomater.* **2009**, *5*, 842; X. Yan, Q. He, K. Wang, L. Duan, Y. Cui, J. Li, *Angew. Chem. Int. Ed.* **2007**, *46*, 2431.
[4] B. H. Kim, D. O. Shin, S.-J. Jeong, C. M. Koo, S. C. Jeon, W. J. Hwang, S. Lee, M. G. Lee, S. O. Kim, *Adv. Mater.* **2008**, *20*, 2303; B. H. Kim, H. M. Lee, J.-H. Lee, S.-W. Son, S.-J. Jeong, S. Lee, D. I. Lee, S. U. Kwak, H. Jeong, H. Shin, J.-B. Yoon, O. D. Lavrentovich, S. O. Kim, *Adv. Funct. Mater.* **2009**, *19*, 2584; D. O. Shin, B. H. Kim, J. H. Kang, S.-J. Jeong, S. H. Park, Y.-H. Lee,

S. O. Kim, *Macromolecules* **2009**, *42*, 1189; S. H. Lee, J. S. Park, B. K. Lim, C. B. Mo, W. J. Lee, J. M. Lee, S. H. Hong, S. O. Kim, *Soft Matter* **2009**, *5*, 2343; S. H. Park, D. O. Shin, B. H. Kim, D. K. Yoon, K. Kim, S. Y. Lee, S.-H. Oh, S.-W. Choi, S. C. Jeon, S. O. Kim, *Soft Matter* **2010**, *6*, 120; B. K. Lim, S. H. Lee, J. S. Park, S. O. Kim, *Macromol. Res.* **2009**, *17*, 666.

[5] D. B. Allerd, A. Cheng, M. Sarikaya, F. Baneyx, D. T. Schwartz, *Nano Lett.* **2008**, *8*, 1434.

[6] L. M. Demers, D. S. Ginger, S. J. Park, Z. Li, S.-W. Chung, C. A. Mirkin, *Science* **2002**, *296*, 1836.

[7] C. L. Haynes, R. P. V. Duyne, *J. Phys. Chem. B* **2001**, *105*, 5599.

[8] Z.-Q. Tian, B. Ren, D.-Y. Wu, *J. Phys. Chem. B* **2002**, *106*, 9463.

[9] K. A. Willets, R. P. V. Duyne, *Annu. Rev. Phys. Chem.* **2007**, *58*, 267.

[10] H. K. Baca, C. Ashley, E. Carnes, D. Lopez, J. Flemming, D. Dunphy, S. Singh, Z. Chen, N. Liu, H. Y. Fan, G. P. López, S. M. Brozik, M. Werner-Washburne, C. J. Brinker, *Science* **2006**, *313*, 337.

[11] J. T. Pelton, L. R. McLean, *Anal. Biochem.* **2000**, *277*, 167.

[12] M. Reches, E. Gazit, *Science* **2003**, *300*, 625.

[13] M. Reches, E. Gazit, *Nat. Nanotechnol.* **2006**, *1*, 195.

[14] T. H. Han, J. Kim, J. S. Park, C. B. Park, H. Ihee, S. O. Kim, *Adv. Mater.* **2007**, *19*, 3924.

[15] T. H. Han, J. K. Oh, J. S. Park, S.-H. Kwon, S.-W. Kim, S. O. Kim, *J. Mater. Chem.* **2009**, *19*, 3512.

[16] J. S. Park, T. H. Han, J. K. Oh, S. O. Kim, *Macromol. Chem. Phys.* **2009**, *210*, 1283.

[17] J. Kim, T. H. Han, Y.-I. Kim, J. S. Park, J. Choi, D. G. Churchill, S. O. Kim, H. Ihee, *Adv. Mater. 22*: **2010**, 583.

[18] M. Reches, E. Gazit, *Nano. Lett.* **2004**, *4*, 581.

[19] X. Yan, Y. Cui, Q. He, K. Wang, J. Li, W. Mu, B. Wang, Z.-C. Ou-yang, *Chem. Eur. J.* **2008**, *14*, 5974.

[20] M. Gupta, A. Bagaria, A. Mishra, P. Mathur, A. Basu, S. Ramakumar, V. S. Chauhan, *Adv. Mater.* **2007**, *19*, 858; X. Yan, Y. Cui, Q. He, K. Wang, J. Li, *Chem. Mater.* **2008**, *20*, 1522.

[21] C. H. Görbitz, *Chem. Eur. J.* **2001**, *7*, 5153.

[22] Gaussian03 (Revision C.02), M. J. Frisch, H. B. Schlegel, G. E. Scuseria, M. A. Robb, J. R. Cheeseman, J. A. Montgomery, Jr., T. Vreven, K. N. Kudin, J. C. Burant, J. M. Millam, S. S. Iyengar, J. Tomasi, V. Barone, B. Mennucci, M. Cossi, G. Scalmani, N. Rega, G. A. Petersson, H. Nakatsuji, M. Hada, M. Ehara, K. Toyota, R. Fukuda, J. Hasegawa, M. Ishida, T. Nakajima, Y. Honda, O. Kitao, H. Nakai, M. Klene, X. Li, J. E. Knox, H. P. Hratchian, J. B. Cross, V. Bakken, C. Adamo, J. Jaramillo, R. Gomperts, R. E. Stratmann, O. Yazyev, A. J. Austin, R. Cammi, C. Pomelli, J. W. Ochterski, P. Y. Ayala, K. Morokuma, G. A. Voth, P. Salvador, J. J. Dannenberg, V. G. Zakrzewski, S. Dapprich, A. D. Daniels, M. C. Strain, O. Farkas, D. K. Malick, A. D. Rabuck, K. Raghavachari, J. B. Foresman, J. V. Ortiz, Q. Cui, A. G. Baboul, S. Clifford, J. Cioslowski, B. B. Stefanov, G. Liu, A. Liashenko, P. Piskorz, I. Komaromi, R. L. Martin, D. J. Fox, T. Keith, M. A. Al-Laham, C. Y. Peng, A. Nanayakkara, M. Challacombe, P. M. W. Gill, B. Johnson, W. Chen, M. W. Wong, C. Gonzalez, J. A. Pople, in *Gaussian, Inc* Wallingford CT **2004**.

[23] M. J. Krysmann, V. Castelletto, A. Kelarakis, I. W. Hamley, R. A. Hule, D. J. Pochan, *Biochemistry* **2008**, *47*, 4597; M. J. Krysmann, V. Castelletto, J. M. E. McKendrick, I. W. Hamley, C. Stain, P. J. F. Harris, *Langmuir* **2008**, *24*, 8158.

[24] V. L. Sedman, L. Adler-Abramovich, S. Allen, E. Gazit, S. J. Tendler, *J. Am. Chem. Soc.* **2006**, *128*, 6903.

[25] N. D. Ednkov, O. D. Velev, P. A. Kralchevsky, I. B. Ivanov, H. Yoshimura, N. Nagayama, *Nature* **1993**, *361*, 26.

[26] Y. Cai, B.-M. Z. Newby, *J. Am. Chem. Soc.* **2008**, *130*, 6076.

[27] A. J. Haes, W. P. Hall, L. Chang, W. L. Klein, R. P. V. Duyne, *Nano Lett.* **2004**, *4*, 1029.

Received: October 30, 2009

